

Finite element modelling of calendering – some aspects of the effects of temperature gradients and structure inhomogeneities

M. WIKSTRÖM, M. RIGDAHL

Swedish Pulp and Paper Research Institute (STFI), Box 5604, S-114 86, Stockholm, Sweden, and Department of Pulp and Paper Chemistry and Technology, Royal Institute of Technology, S-100 44 Stockholm, Sweden

O. STEFFNER

Iggesunds Bruk, S-825 80 Iggesund, Sweden

The compression of a paper web in a calender nip has been simulated using the finite element method. The mechanical properties of the paper were allowed to vary in the thickness and machine directions of the web. This was done in order to model the influence of temperature gradients as well as density variations (due to the presence of fibre flocs) on the deformation behaviour in the nip. Paper was assumed to be an elastic–plastic material exhibiting strain hardening. The yielding behaviour was governed by the Drucker–Prager yield condition. Simulations of the deformation behaviour when paper was subjected to a temperature gradient, clearly revealed that the deformation gradually became more concentrated towards the surface layers as the temperature of the surface increased. This is in accordance with experimental results which indicate that temperature-gradient calendering promotes the surface properties, whereas the bulk of the structure is preserved. Modelling the deformation behaviour of a structure containing density variations reveals that the paper may contain an inhomogeneous strain distribution after unloading, i.e. after passage through the nip.

1. Introduction

One of the purposes of using the soft calendering technique is to produce as good a printing surface as possible with a minimal loss in mechanical properties and bulk of the paper structure. In other words, the aim is to obtain an even compression localized to the surfaces without deforming the inner structure of the paper. The result of the calendering operation is governed by several machine parameters, such as the line load, the temperature of the heated rolls, the dwell time in the nip, the softness of the backing rolls and the shape of the pressure pulse in addition to the properties of the paper. The temperature and moisture content of the paper web are also important in this context.

Using a high roll temperature it is possible to produce a temperature gradient in the thickness direction of the paper at the same time as the paper is compressed in the nip [1, 2]. The high temperature of the paper close to the heated roll surface causes a desirable selective softening that promotes the softening of the surface layers while preserving the interior bulk of the structure. In principle, it is also possible to soften the surface layers by moisture [3], for example by applying water or using steam showers just before the

paper web enters the nip. Gradient calendering techniques have received a great deal of attention during recent years, because they indicate an interesting route to improving the functional properties of the printing paper.

Despite the importance and the long use of the calendering process in the production of paper, the understanding of the compression of the paper structure in the calender nip appears to be, at least partly, insufficient (cf. [4]). To some extent this deficiency is due to a lack of knowledge of the mechanical behaviour of paper structures at large deformations. This is also pointed out in the extensive work of Rodal [5]. It is clear that the calendering of paper poses a quite challenging load case from the mechanical point of view, where the use of numerical simulations could provide advantages. This view has been adopted by Rodal [5] who used the finite element method (FEM) to analyse the deformation of the paper web in the calender nip. However, in that work, no attention was paid to non-uniformities in temperature and structure of the paper. Numerical simulations have also been used to analyse the deformation of the calender rolls in the nip region [6, 7].

In this study, the paper compression in a calender nip was simulated using the finite element method. The paper was modelled as an isotropic elastic-plastic material which is subjected to large strains. The study focused on the structural response of the paper structure compressed in the calender nip, when there are variations in the constitutive parameters caused by heat transfer from the roll surface or by flocs in the paper structure. The results obtained by this FEM technique should be regarded as trends rather than absolute quantitative predictions. This is primarily because there is a lack of knowledge of the mechanical behaviour of paper in the thickness direction under large deformations. When such information is at hand, it should be possible to improve the performance and usefulness of the model considerably.

2. Methods

2.1. General description of the finite element model

The numerical modelling was performed using the commercial finite element software ABAQUS Implicit Version 5.2 [8]. This software was chosen because of the ability of ABAQUS to analyse problems which include large deformations, non-linearities and contacts between dissimilar materials. Another reason was that the program is used world-wide. All calculations were performed with a DEC-station 5240.

Fig. 1a is a schematic drawing of the paper web between two calender rolls. The region where the finite element mesh is generated is shown in Fig. 1b. The left-hand boundary line of this rectangle ("symmetry" line) is thus located exactly beneath the centre of the upper roll, which can be assumed to acquire different temperatures. Fig. 1c provides a magnification of the region in the vicinity of the nip centre. This graph also gives a detailed picture of the mesh used. The mesh is chosen to be denser towards the paper surface in order to provide a more accurate evaluation of the deformation in the region subjected to the thermal gradients. A two-dimensional analysis was performed, i.e. the deformation in the MD (machine direction)-ZD (thickness direction) plane was modelled, whereas no detailed analysis of the deformation in the cross direction (CD) was aimed at. Plane strain conditions were assumed throughout this work when the deformation in the nip was simulated (elements of the CPE8R type were used). The deformation of the paper structure was analysed when it was compressed by the calender roll. There was, however, no dynamic transport of paper into the nip. The paper compression was caused by a prescribed displacement of the roll surface in the thickness direction.

With the ABAQUS software, the stress (and the deformation) field can be evaluated as a function of the thickness reduction in the calender nip up to large deformations. The maximum thickness reduction was 30% in this study. The paper was considered to have a thickness of 200 μm before compression and to be in contact with two similar rolls with radii of 300 mm, see Fig. 1. The calender rolls were regarded as rigid, i.e. having an infinite stiffness. From the geometries of

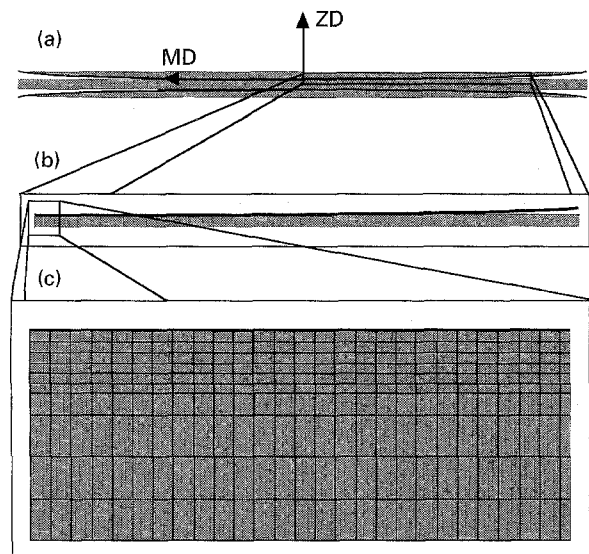


Figure 1 (a) Schematic drawing of the paper between the calender rolls. (b) The region analysed in the FEM simulation. (c) Enlargement of the region in the vicinity of the nip centre showing the finite element mesh.

the roll and the paper, the distance in the MD between the centre of the nip and the point where the paper and the roll were no longer in contact with each other was 4.24 mm when the maximum thickness reduction was 30%.

The increasing contact surface between the upper roll and the paper surface as the roll compresses the paper was controlled by special contact elements of the type IRS22. It was assumed that there was no slip between the roll and the paper. Except for the paper surface in contact with the roll and the symmetry line in the centre of the nip, the whole mesh was allowed to move in the MD.

Further details of the models used in the analysis of the effects of temperature gradients in the thickness direction and structure inhomogeneities are discussed in Section 3.

2.2. Modelling the mechanical behaviour of the paper

When the deformation in the nip was simulated, it was assumed that the paper was isotropic, elastic-plastic with a uniaxial yield stress, σ_0 , and that it exhibited strain hardening after the yield point. Rodal [5] argued that a mechanical model used to describe the plastic deformation in a calendering nip should account for the fact that a void-containing material like paper can undergo permanent volume changes when it is compressed. The von Mises yield condition cannot thus be applied, and Rodal suggested that the Drucker-Prager condition should be used. This condition is also used in this work and is given by

$$A\sigma_m + \sigma_e = B \quad (1)$$

where σ_m is the hydrostatic stress and σ_e the von Mises stress. As in the work of Rodal [5], the Drucker-Prager mean-stress coefficient, A , was chosen to be -0.8571 and the yield-stress coefficient, $B = 0.7423 \sigma_0$.

As has already been pointed out, there is a lack of knowledge about the mechanical behaviour of paper in the thickness direction at large deformations. It was therefore decided to use values of the mechanical parameters at room temperature similar to those used by Rodal [5] as a starting point. The Young's modulus, E , was then set to 690 MPa and the uniaxial yield stress to 6.9 MPa at room temperature. The elastic Poisson's ratio was assumed to be 0.05 and the strain-hardening tangent-modulus $E_T = E/4$. The value of Young's modulus (690 MPa) used here and by Rodal may be regarded as rather high in view of results reported by others (see, for example, [9]).

When temperature-gradient calendering is simulated, the temperature dependence of the mechanical parameters must be accounted for in some manner. Salmén and Back [10] have evaluated the elastic modulus of paper up to high temperatures and these data were used here to simulate the temperature dependence of the Young's modulus, E . The yield stress and the strain-hardening modulus were assumed to vary with temperature in a corresponding way.

Structure inhomogeneities are regarded here as variations in the density of the paper structure. To simulate the effects of the uneven structure of paper on the deformation in the nip, a relation between the Young's modulus and the density, given by Fleischman *et al.* [11], was used. As before, the yield stress and the strain-hardening modulus were assumed to vary with the paper density in a corresponding way.

3. Results and discussion

3.1. Uniaxial compression of the paper at different temperatures

Fig. 2 shows calculated stress-compression curves of paper when compressed between two parallel rigid plates (not in a calender nip) at 20, 150, 200 and 250 °C when the temperature was uniform in the specimens, i.e. no temperature gradients were present. In this case, a plane stress condition was used in the FEM simulation. The structure was deformed plastically already at relatively low loads and it is obvious that the temperature had a non-linear effect on the compression. An

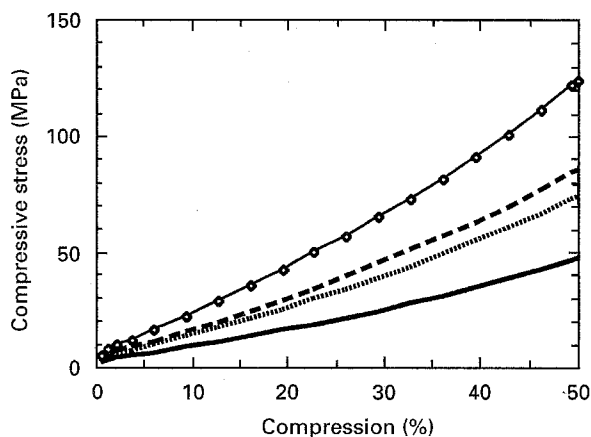


Figure 2 Calculated stress-compression curves for paper compressed between parallel rigid plates. The temperature of the specimens was (\diamond) 20, (---) 150, (... ..) 200 or (—) 250 °C.

increase in temperature from 200 °C to 250 °C produced a larger increase in strain at a given compressive stress than a corresponding increase from 150 °C to 200 °C. This is also evident in Salmén and Back's [10] results on the temperature dependence of the elastic modulus and is the result of a temperature-induced transition (softening) of the material.

3.2. Simulation of temperature-gradient calendering

When the surface of the paper comes into contact with a heated roll in the calender nip, its temperature rises. Owing to the high machine speed and thus the short dwell time in the nip, the temperature will not be uniform in the thickness direction (ZD) but a temperature gradient develops. (In a more realistic case, a temperature gradient also appears in MD. This is discussed later in this section.) The temperature distribution in the z -direction can be estimated by the heat conduction equation, which in the simplest form has the solution [12]

$$T(z, t) = T_0 + (T_s - T_0) \left[1 - \operatorname{erf} \left(\frac{-z}{2(\alpha t)^{1/2}} \right) \right] \quad (2)$$

where T_0 is the temperature of the paper web as it enters the nip, T_s is the temperature of the heated roll, z is the distance to the paper surface, α is the thermal diffusivity of paper and t can be taken as the dwell time from the first contact between the paper and the roll to the centre of the nip. The function $\operatorname{erf}(x)$ denotes the error function. In this case, the thermal diffusivity of the paper was assumed to be $0.116 \times 10^{-3} \text{ mm}^2/10^{-3} \text{ s}$ [2], the temperature of the ingoing web was set to 21 °C and three different values for the temperature of the heated roll were used; 150, 200 and 250 °C. The machine speed of the calender was chosen to be 460 m min^{-1} which corresponds to a dwell time to the centre of the nip of $0.55 \times 10^{-3} \text{ s}$. The temperature distribution in the thickness direction was then calculated using Equation 2. As a starting point, the temperature was assumed to vary only in the z -direction, i.e. variations in the machine direction were not taken into account. The mechanical properties of the paper at a given temperature were evaluated from the data reported by Salmén and Back [10], as outlined earlier. Thus the paper was modelled as a layered structure with its mechanical properties varying in the thickness direction corresponding to the temperature distribution.

Fig. 3 shows the calculated local strain in the z -direction in the paper structure at distances of 5, 25 and 90 μm below the surface in contact with the heated roll and beneath the centre of the roll as a function of the total compression of the paper. "Total compression" here means the compression or deformation of the paper under the centre of the calender roll. Results obtained at the three different temperatures (150, 200 and 250 °C) are included in the graph.

The role of the heated roll is clearly shown in this graph. The deformation in the calender nip was, to a great extent, localized to the softer surface layers of

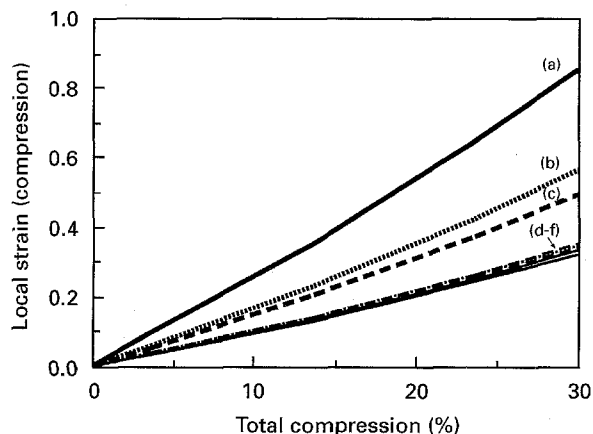


Figure 3 Calculated local strains in the thickness direction for the paper in contact with the heated roll as a function of the total compression of the paper. (a-c) The local strain 5 μm below the paper surface; (d-f) the strain 25 or 90 μm below the paper surface. (—) 250 $^{\circ}\text{C}$, (.....) 200 $^{\circ}\text{C}$, (---) 150 $^{\circ}\text{C}$.

the paper. The strain in the surface layers increased strongly as the temperature increased, i.e. as the temperature gradient became more pronounced. It should also be noted that, when the temperature of the heated roll was raised, the calculated strain in the interior of the structure (25 and 90 μm below the surface) decreased somewhat at a given total compression. Thus an increase in roll temperature had the desired effect of localizing the calendering action to the surface regions and to some extent preserving the bulk structure. The selective nature of the softening of the surface layers is further illustrated by the observation that there were virtually no differences in strain levels at depths of 25 and 90 μm below the paper surface. Before concluding this paragraph, it should be noted that the calculated local strains may be rather high. However, whether strains of this magnitude (up to 0.8) actually can be applied to a fibre network, such as paper, is not discussed here.

Fig. 4 shows the deformed finite element mesh (or rather the calculated compressive strain in the thickness direction) in the region close to the centre of the nip at a total compression of 30% (beneath the centre of the heated roll). In this case, the temperature of the heated roll was set to 250 $^{\circ}\text{C}$. The localized nature of the compression in the thickness direction is apparent.

In Figs 3 and 4, the total strain values are used to illustrate the compression of the structure in the nip. The plastic strain in the z -direction at depths of 5, 25 and 90 μm below the paper surface under the centre of the roll is shown in Fig. 5 as a function of the total compression of the paper. In this case, the temperature of the heated roll was set to 250 $^{\circ}\text{C}$. When the material has yielded, the ratio between the local plastic strain and the local total strain was about 1/3. This was rather independent of the temperature, the distance from centre of the nip and the distance to the paper surface.

In a more realistic situation, a temperature gradient develops not only in the z -direction of the paper, but also in the machine direction from the first contact between the paper surface and the heated roll until the

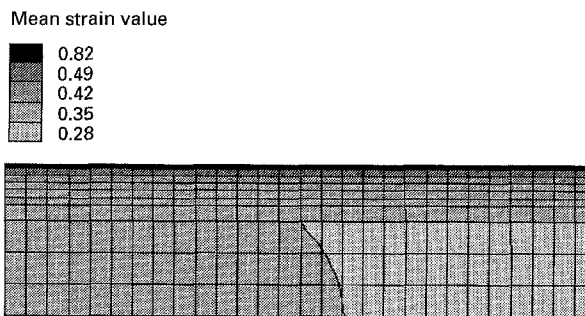


Figure 4 Calculated strain levels in the z -direction in the region close to the centre of the calender nip at a total compression of 30%. The temperature of the heated roll was 250 $^{\circ}\text{C}$.

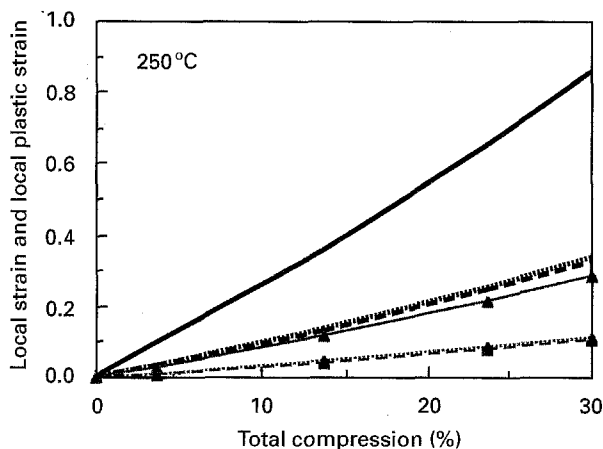


Figure 5 Local total strain and (▲) local plastic strain in the thickness direction at depths of (—) 5, (.....) 25 and (---) 90 μm below the paper surface versus total compression (beneath the centre of the roll) at 250 $^{\circ}\text{C}$.

paper is transported into the centre of the nip. To estimate the effect of the gradient in MD, the paper in the nip was modelled with temperature gradients in both the z -direction and in the MD. The distance in the MD between the centre of the nip and the first contact point with the heated roll was then divided into seven zones with different contact times between the paper surface and the heated roll (0, 0.05, 0.15, 0.25, 0.35, 0.45 and 0.55 ms). For each contact zone, Equation 2 was solved and the corresponding mechanical properties were evaluated. It was, however, found that the temperature gradient in the MD had no significant influence on the calculated deformation close to the centre of the roll. For example, the strain values shown in Fig. 3 were not appreciably affected by the inclusion of the gradient in temperature (and mechanical properties) in the machine direction.

Fig. 6 shows the calculated reaction force in the roll versus the total compression of the paper in the thickness direction. The temperature was 250 $^{\circ}\text{C}$ and two cases were considered. In the first case only the temperature gradient in the z -direction was considered and, in the second case, the gradient in the MD was also incorporated. The two curves almost coincide. The paper had in both cases the same mechanical properties in the region between 0 and 0.8 mm from the centre of the nip. Thus it is, in a sense, the properties of that region that control the deformation in the

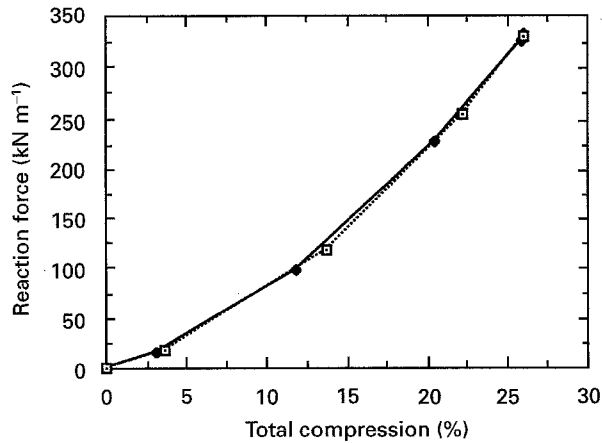


Figure 6 Reaction force in the heated roll versus the total compression of the paper in the thickness direction (□) with and (◆) without the temperature gradient in machine direction. The temperature of the heated roll was 250 °C.

nip and it is the temperature gradient in the thickness direction beneath the centre of the roll that is important in this context.

Fig. 7 shows the calculated stress in the z -direction 25 μm below the surface of the paper as a function of the distance in the MD from the centre of the nip at different roll temperatures. Here only temperature gradients in the z -direction were considered and three temperatures of the heated roll were used in the analysis; 150, 200 and 250 °C. The total compression of the paper in the centre of the nip was set to 30%. When the stress levels at different roll temperatures are compared, it is obvious that the differences were more pronounced close to the centre of the nip, although the stress levels do not actually differ appreciably. The lowest maximum compressive stress was obtained at the highest roll temperature which appears quite reasonable. Similar differences due to the roll temperature were also noted when evaluating the reaction force in the roll.

The stress distribution predicted by the contact theory of Hertz is given by [13]

$$\sigma_z(y) = \sigma_H \left(1 - \frac{y^2}{a^2}\right)^{1/2} \quad (3)$$

where σ_H is the maximum compressive stress in the nip, $2a$ is the nip length, σ_z is the compressive stress in the thickness direction and y is the distance to the centre of the nip ($0 \leq y \leq a$). The prediction of the equation is included in Fig. 7, where $\sigma_H = 160$ MPa and $2a = 8.4$ mm. The stress distributions obtained from the finite element analysis do not coincide with that predicted by the Hertz theory. Equation 3 predicts, in general, a higher stress at a given distance from the nip centre than the FEM analysis. This difference may not be unexpected, because the Hertz equation is based on linear elasticity and it actually refers only to the stress distribution in the contact region when two rolls are forced together, i.e. without any paper which could deform plastically between them. Keller [14] measured the stress distribution in the nip between two contacting rolls without any paper between them. He actually noted that the pre-

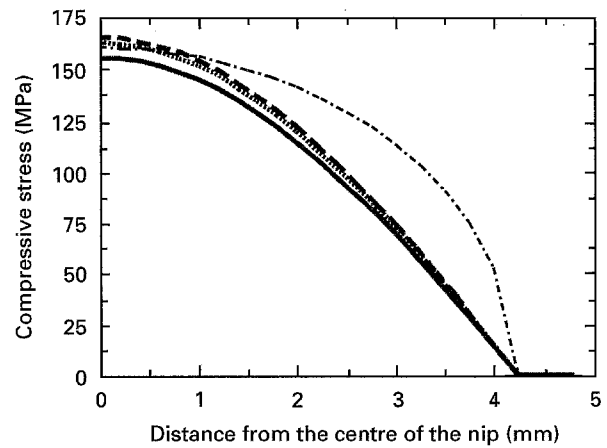


Figure 7 Calculated stress levels in the z -direction 25 μm below the surface from the centre of the nip until the paper is no longer in contact with the roll. The total compression of the paper under the roll was 30%. The temperature of the heated roll was (---) 150, (....) 200 or (—) 250 °C. The prediction of the Hertz theory is also included in the figure (-.-.-).

diction of the Hertz theory overestimated the measured stress value over most of the nip region.

The shear stresses in the paper in the calender nip can also be evaluated with the FEM technique used here. As was also reported by Rodal [5], all shear stresses were found to be small in comparison with the compressive stresses in the thickness direction. They were close to zero in the centre of the nip and they then increased with increasing distance from the centre of the nip. The maximum values, of the order of 2–3 MPa, were noted in the region where the paper lost contact with the heated roll. It should be stressed that these results were obtained when a non-moving paper web was considered to be compressed by a stiff roll. The situation might be different if dynamic effects were taken into account, i.e. if the paper web was allowed to pass through the nip with a certain velocity.

3.3. Simulation of calendering of an inhomogeneous paper structure

It is well-known that paper is an inhomogeneous material and that its local density varies. The variation in density is also reflected in a corresponding variation in the mechanical properties of the material. The uneven structure of paper is often described in terms of a floc structure and different formation concepts [15]. The uneven character of the paper structure is also of consequence for the calendering operation. Owing to the variations in mechanical properties and in the local thickness of the paper, the deformation in the calender nip will not be uniform and the calendering may even accentuate the unevenness in structure and properties [16], e.g. an undesired variation in gloss may be evident after the calendering. It is thus important to improve the understanding of the effect of the inhomogeneities in structure on the local deformation in the calender nip. The finite element method appears to be quite well suited to provide this type of knowledge.

In accordance with earlier reported results [17], it was assumed here that the density of the paper varied between 800 and 900 kg m⁻³. The relation between the Young's modulus and the density reported by Fleischman *et al.* [11] was then used (after normalization with the value of the modulus suggested by Rodal [5]) to produce a model of a paper structure with varying mechanical properties. The yield stress and the strain-hardening tangent-modulus were also assumed to vary in the MD-ZD plane in a manner corresponding to the variation in the paper density. Fig. 8 shows a part of the FEM model used for the simulation. It represents an attempt to model the floc character of the paper, and the Young's modulus, E , was assumed to vary between 544 and 768 MPa. The average value of E was, as before, 690 MPa. In Fig. 8, a floc is located exactly beneath the centre of the calender roll. In general, the surface regions were modelled as low-density regions with lower values of the mechanical parameters.

The maximum compression of the paper was set to 30% and the temperature to 20°C. When modelling the deformation in the nip, the roll was no longer used for the compression. It was instead assumed that the upper paper surface was compressed to the same extent along the entire length of the

model (actually compressed between two parallel plates). This simplification is only relevant when the region close to the centre of the nip is analysed. The length of the model was here chosen to be 2 mm (1 + 1 mm with a symmetry line in the middle of the floc). Fig. 9 illustrates the stresses (in the z-direction) in the structure when the paper was compressed 30%. The stresses were highest in the regions of higher density, i.e. the floc region. It is these regions that have the highest Young's modulus (and yield stress), and the plastic flow after the yield point is apparently insufficient to equalize the stress distribution throughout the structure. This inhomogeneous loading of the structure can enhance the uneven character of the paper. Flocs may even be crushed due to the load concentration, and this may lead to an unevenness in appearance.

Because the inhomogeneous paper was assumed to deform in a plastic manner during the calendering operation, it may be expected that it may contain an inhomogeneous strain (and residual stress) field after the calendering. With the software used here, the paper structure may be unloaded after an initial deformation and the resulting stress or strain distribution in the unloaded structure calculated. Fig. 10 provides one example of this, using the same inhomogeneous



Figure 8 Model of the inhomogeneous paper structure used in the simulations.



Figure 9 Calculated stresses in the thickness direction in an inhomogeneous paper structure. The paper model was compressed 30%.

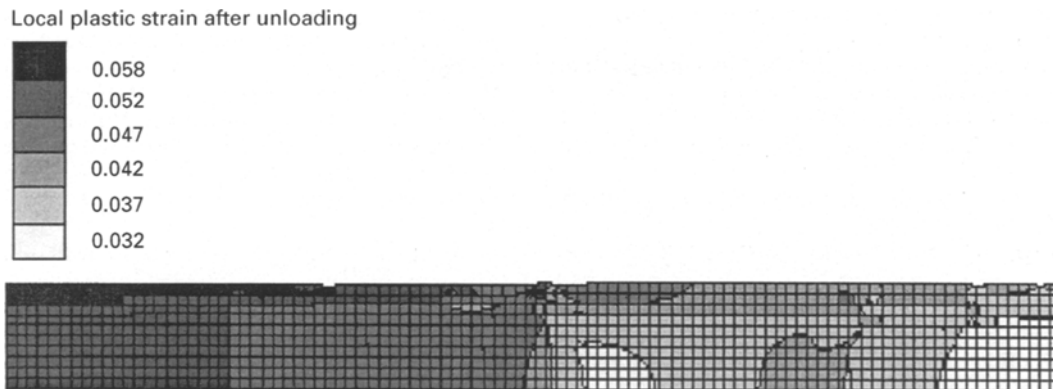


Figure 10 Calculated local plastic strains in the thickness direction in an inhomogeneous paper structure after unloading. The paper model was first compressed 30% and then unloaded.

paper structure as before. The paper was first compressed 30% and then unloaded and allowed to recover until the reaction force in the surface nodes of the finite element mesh was zero, resulting in a permanent deformation of the paper. (No attempt was made here to match the calculated permanent thickness reduction with that obtained in a real calendering situation. To make such a comparison a more accurate estimation of the mechanical properties in the thickness direction is required.) The resulting distribution of the plastic strain (in the thickness direction) is given in the figure.

The calculated local strains (and the corresponding residual stresses) after the unloading, vary throughout the structure due to its uneven character. It is evident that the high-density regions, i.e. the flocs, are in this case subjected to the largest plastic strains after the calendering operation. If the residual stresses, for some reason, are partly released, the paper will probably deform, but this recovery may not be homogeneous throughout the structure. This has also, to some extent, been observed in practice. If a paper is calendered before it is coated, stresses can be built into the structure due to the calendering. When the paper is then coated, the contact with the liquid phase of the coating colour releases the residual stresses and a "roughening" of the surface of the base paper under the not yet consolidated coating layer, takes place [18, 19]. This surface movement has been reported to occur on the floc size level and can redistribute the mass of the coating layer in a negative way leading to a mottled offset print. This undesired effect is caused by the inhomogeneous stress (or strain) field built into the structure by the calendering.

4. Final remarks

It is evident that the finite element method can be of great value in an analysis of the deformation of paper structures in a calender nip. This appears to be especially true if the inhomogeneous nature of paper must be taken into account. The objective of this work was merely to outline how the rather complex deformation behaviour of such materials in the calender nip could be analysed. It is intended to refine the modelling in

future work and also to make a comparison with the results of experimental trials.

It is also clear from the work reported here that there is a lack of material data and knowledge of how to describe the deformation of paper in the thickness direction. The Drucker-Prager yield condition has been used here, but it is not known whether this relation is the best suited for paper. There are, furthermore, only few studies which report on yield stress, Young's modulus, strain-hardening, etc., in the thickness direction. This kind of information is required if the full potential of techniques such as FEM are to be used. Furthermore, it is certainly desirable to model the dynamic compression of the paper in the nip. In such a case, it would be necessary to account for the viscoelastic nature of paper. To accomplish this, more experimental work dealing with the mechanical description of paper is required.

Acknowledgements

The authors thank Mr Lars Delhage, Department of Solid Mechanics, Royal Institute of Technology, for valuable advice on the numerical simulations, and the Computer group at STFI for help with the software. Thanks are also extended to Dr J. A. Bristow for the linguistic revision of the manuscript. The financial support from "Stiftelsen Cellulosa- och Pappersforskning" is gratefully acknowledged.

References

1. R. H. CROTOGINO, *Tappi J.* **65**(10) (1982) 97.
2. J. H. VREELAND, K. B. JEWITT and E. R. ELLIS, in "Proceedings of the Tappi Coating Conference", (Tappi Press, Atlanta, 1989) p. 179.
3. R. H. CROTOGINO and M. F. GRATTON, in "Proceedings of the Tappi Paper Physics Conference", (Tappi Press, Atlanta, 1987) p. 199.
4. J. D. PEEL, in "Transactions of the IXth Fundamental Research Symposium", Cambridge, Vol. 2 edited by C. F. Baker (Mechanical Engineering Publications, London, 1989) p. 979.
5. J. J. A. RODAL, *Tappi J.* **76**(12) (1993) 63.
6. J. J. A. RODAL, in "Transactions of the IXth Fundamental Research Symposium", Cambridge, Vol. 2 edited by C. F. Baker (Mechanical Engineering Publications, London, 1989) p. 1055.
7. R. H. MOORE and C. C. MOSCHEL, *Tappi J.* **77**(3) (1994) 117.

8. ABAQUS (Hibbitt, Karlsson and Sorensen, Inc., Version 5.2, Rhode Island, 1992).
9. G. A. BAUM, in "Transactions of the Xth Fundamental Research Symposium", Oxford, Vol. 1 edited by C. F. Baker (Pira International, Leatherhead, 1993) p. 52.
10. N. L. SALMÉN and E. L. BACK, *Sv. Papperstidn.* **81** (1978) 341.
11. E. H. FLEISCHMAN, G. A. BAUM and C. C. HABEGER, *Tappi J.* **65**(10) (1982) 115.
12. J. P. HOLMAN, "Heat Transfer" (McGraw-Hill, New York, 1976).
13. J. PAV and P. SVENKA, *Das Papier* **39**(10A) (1985) V178.
14. S. F. KELLER, in "Proceedings of 77th Annual Meeting of the Technical Section CPPA", (Technical Section, Canadian Pulp and Paper Association, Montreal, 1991) p. B89.
15. B. NORMAN, in "Paper Structure and Properties", edited by J. A. Bristow and P. Kolseth (Marcel Dekker, New York, 1986) p. 132.
16. I. M. KAJANTO, *Paperi ja Puu* **72** (1990) 600.
17. O. STEFFNER, Lic. Eng. thesis, Department of Pulp and Paper Chemistry and Technology, Royal Institute of Technology, Stockholm (1993).
18. G. ENGSTRÖM and J.-F. LAFAYE, *Tappi J.* **75**(8) (1992) 117.
19. J. SKOWRONSKI, *J. Pulp Paper Sci.* **16**(3) (1990) J102.

*Received 8 August
and accepted 21 December 1995*